

Evaluation of Jet Noise Sources by Cross-Correlation of Far Field Microphone Signals

S. P. PARTHASARATHY*

Jet Propulsion Laboratory, Pasadena, Calif.

The objective of this paper is the evaluation of the noise sources from the far field measurements of jet noise. A one-dimensional model is envisioned in which noise sources move along the axis of the jet downstream of the nozzle. The autocorrelation function of the noise sources in the moving frame of reference is a function of time and time delay. A theory is developed for stationary sources and then extended to moving sources. The method of obtaining the autocorrelation through a least squares inversion method is illustrated for a high-temperature subsonic jet flow. This method can be extended to supersonic flows.

Nomenclature

A, B	= position of noise source
$A_{ijkl}, \tilde{A}_{ijkl}$ $B_{ijkl}, \tilde{B}_{ijkl}$ $C_{ijkl}, \tilde{C}_{ijkl}$	= correlation functions, Eqs. (17-25)
c	= velocity of sound
C	= cross-correlation function Eq. (10)
E	= position of noise sources
f	= frequency
g	= a function of time, Eq. (12)
i, j, k, l	= indices
M	= Mach number, scalar
\mathbf{M}	= Mach number, vector
M_1, M_2	= microphones
n	= number of sources emitted per unit time
N_1	= number of bands
N_2	= number of nodal points
0	= position, see Fig. 6
p	= sound pressure
r	= distance
s	= source strength, $(\rho_0/4\pi)(d^2v/dt^2)$
t, t', t_p	= times
T_{ij}, \tilde{T}_{ij}	= acoustic stress tensor
V	= velocity of noise source
v	= fluctuating volume of noise source
x, y, z	= position coordinates of microphones
\mathbf{X}, \mathbf{X}^*	= position vectors of field points
\mathbf{Y}, \mathbf{Y}^*	= position vectors of source points
\mathbf{Y}_1	= the vector $(Y_1, 0, 0)$
Y_1	= position coordinate on the axis of motion
α	= ratio of maximum frequency to minimum frequency in a band
δ	= time increment
ζ, η	= position vectors of source points
θ, θ^*	= angles between the radius vectors and the axis of motion, see Fig. 6
λ	= wavelength of sound
ρ	= density
τ	= time delay

ϕ = autocorrelation function of noise of a particular bandwidth, Eq. (13)

Ψ = convected auto-correlation

Subscripts

0	= refers to the first zero crossing of the auto-correlation function, see Fig. 2
1, 2, 3, 4	= refers to specific microphones or noise sources
+ and -	= refers to forward and backward waves in supersonic motion
i, j, k, l	= tensor subscripts
i	= index
o	= refers to the ambient medium in which sound is propagated
s	= refers to source
e	= refers to emission time
$\langle \rangle$	= average
$()$	= function of
$[], \{ \}$	= products
\sim	= quantities described in η, t_e coordinates
—	= overbar indicates average in the figures

Introduction

A NOISE source produces random waves of sound. The source can be described by its autocorrelation function or its spectrum. The problem considered here is the evaluation of the autocorrelation functions of many spatially separated sources.

A microphone placed in a noise field responds to the sound pressure on its diaphragm. If the noise field is caused by a number of sources, the microphone cannot isolate the sound pressure levels from each source but can only measure the total sound pressure produced by all sources. There will be an effect of directionality in the sense that the microphone responds to sounds from certain directions more than from others, but usually microphones are comparatively omnidirectional. Specially constructed directional microphones can be used to locate and measure apparent sources of noise but they have the disadvantage that their directional response varies with the frequency. For example, the tubular directional microphone described by Mason and Marshall¹ has a field of view of 30° at 1000 Hz. However, the field of view narrows at higher frequencies and broadens at lower frequencies. Another device which is frequently dependent is the parabolic reflector with a microphone located at the focus. For example, a reflector which had a diameter of 98 cm and a radius of curvature of 100 cm was used by Grosche² for measurements of jet noise. Its half-width was equal to 1.2 λ where λ is the wavelength of sound. This means, for example, that this mirror will resolve two sound sources located a minimum of 5 cm apart at 8 kHz, or a minimum of 10 cm apart at 4 kHz, and so on. If the sources are close together, they will appear as a single source.

Presented as Paper 73-186 at the AIAA 11th Aerospace Sciences Meeting, Washington, D.C., January 10-12, 1973; received January 19, 1973; revision received November 1, 1973. This work presents the results of one phase of research carried out in the Propulsion Research and Advanced Concepts Section of the Jet Propulsion Laboratory, California Institute of Technology, under Contract NAS7-100, sponsored by NASA. The development of the computer program by R. Cuffel which was used to obtain the calculated results and the many discussions held with P. Massier regarding this task are greatly appreciated.

Index category: Aircraft Noise, Aerodynamics (Including Sonic Boom).

* Senior Scientist. Member AIAA.

A large sensitivity to direction may be obtained by using two microphones to obtain the cross-correlation. This is done by multiplying the two signals and averaging the product over a period of time. If the source is located at the same distance from the microphones, the signals received by each will be identical because the same wavefront reaches both microphones at the same time. In this case, the cross-correlation will be a maximum. If, however, the source is not located on this line of symmetry, different wavefronts reach the microphones at the same time and the cross-correlation will be greatly reduced. The two microphones therefore detect sources near the line of symmetry. By this method, single sources can be isolated when many sources are present as will be shown in the next section.

The actual field of view in the correlation method depends on how small the autocorrelation width of the source is compared to the time delays that can be obtained by separating the two microphones. On this basis, for measurements made in a room where the microphone separation is of the order of 1 m, a resolution of a few cm is obtained for noise sources with an autocorrelation time of about a tenth of an msec. The resolution of the microphone pair depends on the bandwidth of the noise sources, but the method is free from the irregular frequency response of the tubular type or the steeply rising response of the reflector. It must be pointed out that the correlation method is applicable for random noise sources only as distinguished from sources of speech or music. Also, the actual signal from one noise source is not available separately when many noise sources are present. However, its autocorrelation function can be found. In the tubular type or the reflector, the actual signal is available and this is useful for isolating sources of noise, speech, or music and discriminating against other sources around the microphone.

In the past, apparent noise sources have been located from the contours of equal intensity of noise filtered in a certain band. This can be done by drawing lines through geometrically similar points on the contour lines in the far field and extending them to the jet axis. Usually, a single straight line cutting the contours at right angles will be sufficient. Lighthill quotes examples of this procedure from the work of Gerrard⁴ and from Westley and Lilley.⁵ The common perpendicular cannot be drawn with great accuracy and in any case the noise source is not located at any point on the axis but has a finite extent.

Yu and Dosanjh⁶ explored the near and far field of supersonic jets in detail and took the position of apparent sources to be the origin of the contour lines of equal sound pressure. This is the same location as would be measured by traversing a microphone on the jet boundary. In general, measurements near the jet contain sound other than the radiated sound and the location of maximum sound pressure along the jet boundary does not agree with the location shown by the common perpendicular. The same data was used by Tam⁷ to locate two apparent sources situated about 7 and 16 diam downstream of the nozzle, whereas the near field contours were centered at about 16 diam downstream.

Bishop et al.⁸ aimed a hot high-speed jet through a small hole in a sound absorbing screen. The hole was large enough that it did not interfere with the jet structure but small enough that it allowed only a small amount of noise to pass through from one side to the other. A microphone located on the side far from the jet responds to noise from the "visible" part of the

jet. From the spectra obtained with the screen located at various distances downstream of the jet exit, the source distribution can be inferred. They point out that the method is not suitable in low speed flows where the screen can interact with the near field to generate new sound sources.

Dyer⁹ showed that the axial distribution of sound power in a turbulent jet can be determined simply in terms of the spectrum of the radiated power and the frequency of the sources as a function of location along the jet axis. The assumed unique relation between the frequency of the sound and its location is to be obtained by a method such as drawing a common perpendicular to the filtered sound pressure contours far from the jet. In his paper Dyer used the data of Howes and Mull¹⁰ where the source location technique was simply a measurement of the sound pressure filtered in $\frac{1}{3}$ octaves along the jet boundary (i.e., the near field). In general, the peak sound pressure on the jet boundary occurs at a different location from the position of the apparent source located by using the far field contours.

Maestrello¹¹ and McDaid traced the source regions of a subsonic cold jet by measuring narrow band space correlations on a plane rigid surface located in the vicinity of the jet. In this method a wave vector decomposition of radiated sound is used and it appears to be applicable without the rigid plate which reflects sound. They noted that the observed nonhomogeneity of the sound field over the plate presents both experimental and conceptual difficulties in this method.

Mollo-Christensen¹² measured space-time correlations of pressure fluctuations in the immediate vicinity of the jets. The idea was to determine whether the near field pressure fluctuations could be interpreted as the source for radiated noise with the jet being modelled as a semi-infinite antenna for sound. This was not carried out but several interesting properties of the near field pressure correlations were measured.

In the present method of source location, the velocity of the moving sources is assumed to be given. In the model, point sources which move along the jet axis are considered. The medium in which sound propagates is assumed to be at rest everywhere. Thus, refraction phenomena are neglected. A more realistic model would be one in which a source moves within a slug flow. This requires a more complex formulation and has not been considered in this paper. Furthermore, determination of the moving autocorrelation depends on an inversion of measured cross-correlations. This inversion cannot be accomplished with great accuracy because of the amount of computation involved.

Theory of the Correlation Method for Locating Stationary Noise Sources

First, for simplicity, consider the arrangement of two microphones M_1 and M_2 located at distances r_{31} , r_{41} , r_{32} , r_{42} from two noise sources s_3 and s_4 as shown in Fig. 1. The sources s_3 and s_4 are assumed to be simple (monopole) sources which radiate sound uniformly in all directions.

A small fluctuating volume v radiates sound according to the simple formula

$$p(t) = \frac{\rho_0}{4\pi r} \frac{d^2 v}{dt^2} \left(t - \frac{r}{c} \right) \quad (1)$$

In all of the equations the parentheses $()$ denote "a function"; whereas, the $[\]$ denote "multiplied by." The quantity $v(t)$, v a function of t , is the fluctuating volume of the source, ρ_0 is the mean density of the propagation medium, r is the distance from the source to the location at which $p(t)$, the fluctuating pressure, is being measured, and c is the velocity of sound of the medium through which the sound is propagating. The quantity $d^2 v/dt^2 (t-r/c)$ is the second time derivative of the volume taken at the retarded time $(t-r/c)$ because the pressure wave measured at time t at the measuring station was produced at the source at a prior time $(t-r/c)$.

The energy flux density due to the sound wave is given by the mean value of the square of the pressure

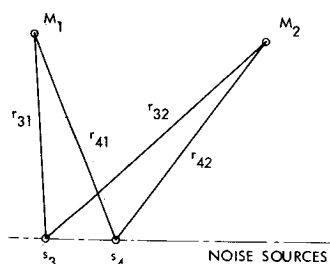
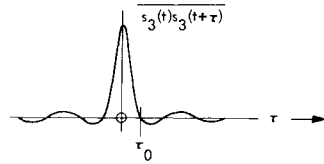


Fig. 1 Two noise sources and two microphones.

Fig. 2 Autocorrelation of source s_3 vs time delay.



$$\frac{\langle p^2 \rangle}{\rho_o c} = \frac{1}{\rho_o c} \left\langle \left[\frac{\rho_o}{4\pi r} \frac{d^2 v}{dt^2} \left(t - \frac{r}{c} \right) \right]^2 \right\rangle \quad (2)$$

or

$$\frac{\langle p^2 \rangle}{\rho_o c} = \frac{\rho_o}{16\pi^2 c r^2} \left\langle \left[\frac{d^2 v}{dt^2} \right]^2 \right\rangle$$

Equation (2) is an expression of the inverse square law. The total energy radiated by the source per unit time is $4\pi r^2$ times the flux density; hence, the total radiated energy is

$$\frac{\rho_o}{4\pi c} \left\langle \left[\frac{d^2 v}{dt^2} \right]^2 \right\rangle$$

This total radiated energy is generally defined as the strength of the source. For the discussion that follows, however, it is convenient to consider the quantity $\rho_o/4\pi d^2 v/dt^2$ [in Eq. (1)] as the source strength s of the pressure wave so that the sound pressure is

$$p(t) = [s(t-r/c)]/r \quad (3)$$

For the configuration of Fig. 1, the sound pressure at each of the two microphones is therefore given by the superposition of the sound pressure fields at the location of the microphone caused by two sources s_3 and s_4 . Thus, at location M_1

$$p_1(t) = \frac{s_3(t-r_{31}/c)}{r_{31}} + \frac{s_4(t-r_{41}/c)}{r_{41}} \quad (4)$$

At location M_2

$$p_2(t) = \frac{s_3(t-r_{32}/c)}{r_{32}} + \frac{s_4(t-r_{42}/c)}{r_{42}} \quad (5)$$

The quantities $s_3(t)$ and $s_4(t)$ are the strengths of the two sources. If, now, a time delay τ is introduced in the observed signal at location M_1

$$p_1(t-\tau) = \frac{s_3(t-(r_{31}/c)-\tau)}{r_{31}} + \frac{s_4(t-(r_{41}/c)-\tau)}{r_{41}} \quad (6)$$

In addition, if Eq. (6) is multiplied by $p_2(t)$, given by Eq. (5), and averaged over t

$$\begin{aligned} \langle p_1(t-\tau)p_2(t) \rangle &= \left\langle s_3 \left(t - \tau - \frac{r_{31}}{c} \right) s_3 \left(t - \frac{r_{32}}{c} \right) \right\rangle / r_{31}r_{32} + \\ &\left\langle s_4 \left(t - \tau - \frac{r_{41}}{c} \right) s_4 \left(t - \frac{r_{42}}{c} \right) \right\rangle / r_{42}r_{41} + \\ &\left\langle s_3 \left(t - \tau - \frac{r_{31}}{c} \right) s_4 \left(t - \frac{r_{42}}{c} \right) \right\rangle / r_{31}r_{42} + \\ &\left\langle s_4 \left(t - \tau - \frac{r_{41}}{c} \right) s_3 \left(t - \frac{r_{32}}{c} \right) \right\rangle / r_{32}r_{41} \end{aligned} \quad (7)$$

The correlation $\langle s_3(t)s_3(t+\tau) \rangle$ of the source strength $s_3(t)$ at time t with the same source strength $s_3(t+\tau)$ at a different

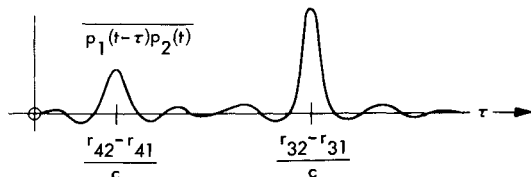


Fig. 3 Cross-correlation of the pressures: good resolution.

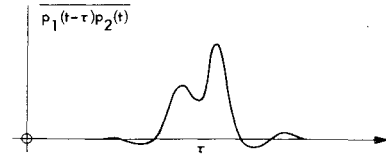


Fig. 4 Cross-correlation of the pressures: poor resolution.

time $(t+\tau)$ is defined as the autocorrelation function of the source s_3 . This correlation depends only on the time difference τ and not on both t and τ for a source strength which is statistically stationary. It has a peak at $\tau = 0$, is symmetric about $\tau = 0$, and for a wideband noise, is significant only near $\tau = 0$ as shown in Fig. 2. The value τ_o at which the autocorrelation function nearest the vertical axis is zero defines the time delay scale. τ_o is inversely proportional to the bandwidth. The power spectrum of s_3 is the Fourier transform of the autocorrelation function $\langle s_3(t)s_3(t+\tau) \rangle$. The autocorrelation function of s_4 is similar to that of s_3 , the exact shape depending on the character of its noise.

Next, assume that the noise sources are uncorrelated, that is, the sources are independent of each other. For example, two loud speakers are energized by two different noise generators. Then the last two terms in Eq. (7), which are the cross-correlation terms, are zero because the average value of two independently random fluctuating quantities is zero. The first two terms in Eq. (7), however, do not vanish. If the cross-correlation of the sound pressures from the two microphones [the left-hand side of Eq. (7)] is obtained experimentally and plotted as a function of τ , a graph like the one in Fig. 3 or the one in Fig. 4 results. Figure 3 corresponds to the case in which the difference between $[r_{42}-r_{41}]/c$ and $[r_{32}-r_{31}]/c$ is large compared to the larger of the autocorrelation scales of s_3 and s_4 . In Fig. 4 the preceding difference is small and is of the order of τ_o or less.

In Fig. 3 the first peak occurs at $\tau+r_{41}/c=r_{42}/c$ where the second term in Eq. (7) has a maximum value equal to

$$\left\langle s_4^2 \left(t - \frac{r_{42}}{c} \right) \right\rangle / r_{42}r_{41} \quad \text{or} \quad \langle s_4^2 \rangle / r_{42}r_{41}$$

This quantity is merely the mean square of the strength of source 4 divided by $r_{42}r_{41}$. Similarly, at $\tau+r_{31}/c=r_{32}/c$ the peak of the mean square of the other strength $\langle s_3^2 \rangle / r_{31}r_{32}$ appears. In this case the identity of the two noise sources is clearly established because the two peaks in Fig. 3 are well separated and the cross-correlation function $\langle p_1(t-\tau)p_2(t) \rangle$ essentially displays the individual autocorrelation functions of the sources located at different positions on the τ axis. Thus, spatial separation of the sources results in a time delay separation of the autocorrelation functions of the sources. When the resolution is poor, the functions overlap as in Fig. 4 or perhaps even only one peak is observed. In order to separate the individual autocorrelations, it is necessary to increase the distance between the two microphones. If this is not possible the sources must be treated together as one.

If the sources are now considered to be correlated [that is, the cross terms in Eq. (7) exist] instead of being uncorrelated as was assumed previously, there will be additional peaks between the two shown in Fig. 3. These additional peaks result from the last two terms in Eq. (7). Figure 5 shows this case for the condition for which the peaks are well separated.

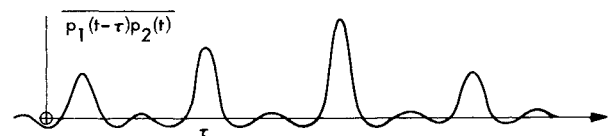


Fig. 5 Cross-correlation of the pressures when the sources are correlated: good resolution.

It should be noted that two equal fully correlated sources produce the same correlation curve as four equally strong, uncorrelated sources and the interpretation becomes ambiguous. Without additional information about the sources or about the noise field, it is difficult to locate and determine auto-correlations of the correlated sources.

In applying the correlation method to noise radiated from jets where it is suspected that different parts of the jet may be correlated (because a source moves with the flow and retains its identity for a period of time), a formulation which accounts for this correlation in the beginning is more useful. In this case the formulation would be for uncorrelated sources in motion which will be considered in the next section.

The preceding discussion pertained to discrete stationary sources. For completeness Eq. (7) is extended to the case of a distribution of uncorrelated stationary sources located along a line which will be designated as the x axis. If Ψdx is the mean square of the strength in the interval dx , replacement of $\Sigma \langle s(s) \rangle$ in Eq. (7) by $\int \Psi dx$ leads to

$$\langle p_1(t-\tau)p_2(t) \rangle = \int_0^\infty \frac{\Psi \left(x, \tau + \frac{r_1(x)}{c} - \frac{r_2(x)}{c} \right) dx}{r_1(x)r_2(x)} \quad (8)$$

Theory of the Correlation Method for Noise Sources in Motion

The following analysis pertains to an extension of the correlation method for locating stationary noise sources to that of noise sources which are moving. The noise sources in a jet, for example, are considered to be moving eddies; hence, their motion must be accounted for in order to properly interpret the noise generation mechanisms from the data obtained with microphones that are stationary. The first part of the analysis will be devoted to sources moving at subsonic velocities and then the relations for supersonic motion will also be given.

The following analysis is for point monopole sources moving along the axis of the jet. In the appendix, however the modification necessary for a volume distribution is considered.

1. Noise Sources Moving at Subsonic Velocities

Consider monopole noise sources which are produced at some point 0 and move with a uniform subsonic velocity V along the x axis as shown in Fig. 6. The sound pressure at O_1 (more than a few wavelengths from the source) caused by a source of strength s is given by Morse and Ingard¹³

$$p_1(x_1, y_1, z_1, t) = \frac{s(t - (r_1/c)(t))}{r_1(t)[1 - M \cos \theta_1(t)]^2} \quad (9)$$

The quantity $s(t)$ is the strength of the moving random noise source. It is also the total rate of change of mass flux out of the monopole source; r_1 is the distance from the point of emission to the observation point O_1 ; t_e is the emission time of the wave which travels to O_1 from the source when it is at point A.

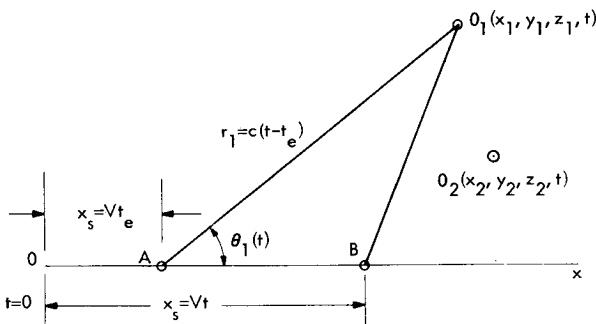


Fig. 6 A noise source in subsonic motion.

When the wave reaches point O_1 , the source will be at point B. $M = V/c$ where c is the speed of sound in the medium through which the sound is propagated and θ_1 is the angle between AO_1 and the x axis. A similar expression gives the sound pressure at O_2 . O_1 and O_2 indicate positions of two microphones. The distance r_1 and the angle θ_1 are functions of t . The quantity $s(t - r_1(t)/c)$ is s taken at the retarded time $t - r_1(t)/c$. In the preceding arrangement, the sound wave emitted at some point on the x axis reaches O_1 first and O_2 later. If a time delay τ is introduced artificially in the signal p_1 , it may be shown that the cross-correlation between the sound pressures at O_1 and O_2 are

$$E\{p_1(t-\tau)p_2(t)\} = E\left\{ \frac{s(t-\tau-(r_1/c)(t-\tau))s(t-(r_2/c)(t))}{r_1(t-\tau)[1-M\cos\theta_1(t-\tau)]^2 r_2(t)[1-M\cos\theta_2(t)]^2} \right\}$$

$E\{\}$ represents the ensemble average of the random variable contained in the brackets. This quantity is a function of both t and τ . If Ψ is the noise autocorrelation function equal to $E\{s(t_1)s(t_2)\}$ which is equal to $\Psi(t_1, t_2)$, the above expectation value (average value for a random process) is

$$\frac{\Psi(t-\tau-(r_1/c)(t-\tau), t-(r_2/c)(t))}{r_1(t-\tau)[1-M\cos\theta_1(t-\tau)]^2 r_2(t)[1-M\cos\theta_2(t)]^2}$$

Ψ is also a function of t and τ which means that the noise source represents a nonstationary random process. It is the autocorrelation measured by an observer moving with the source. Thus Ψ is the autocorrelation of the quantity $s(t)$ which is equal to the limit as $r_1 \rightarrow 0$ of $r_1 p_1(x, t)$ with x being chosen at 90° to the axis of motion where the factor $[1 - M \cos \theta]$ is unity. The quantity obtained from the microphone measurements is the time average of the product of the signals of O_1 and O_2 and this is related to the previous expectation value.

If in an actual sound producing medium n sources are produced per unit time at 0 and they move with a uniform velocity, the experimentally determined cross-correlation is $C(\tau)$, which may be expressed as

$$C(\tau) = n \int_{T_1+\tau}^{T_2} \frac{\Psi(t-\tau-(r_1/c)(t-\tau), t-(r_2/c)(t)) dt}{r_1(t-\tau)[1-M\cos\theta_1(t-\tau)]^2 r_2(t)[1-M\cos\theta_2(t)]^2} \quad (10)$$

$$\begin{aligned} &T_2 \quad \text{if } T_2 > T_1 + \tau \\ &\quad \text{lower limits of integration} \\ &T_1 + \tau \quad \text{if } T_2 < T_1 + \tau \end{aligned}$$

In the lower limit of integration T_1 or T_2 is the time taken for sound waves to travel from 0 to O_1 and from 0 to O_2 , respectively.

The derivation of Eq. (10) can be clarified with the use of sketches. The signals $p_1(t)$, $p_2(t)$, and the delayed signal $p_1(t-\tau)$ are shown in Fig. 7 for the case $T_2 > T_1 + \tau$. The expectation value of the product of the sound pressures is shown also.

The signals measured by the microphones at O_1 and O_2 are stationary (statistical properties independent of time) because they are produced by a succession of pulses such as $p_1(t)$ in Fig. 7. These pulses are caused by noise sources emitted from the origin 0 at an average rate n/sec . The experimentally evaluated cross-correlation may be imagined to be the sum of the individual ones of which a sample is $E\{p_1(t-\tau)p_2(t)\}$ shown in Fig. 7. Thus, n times the time average of the function $E\{p_1(t-\tau)p_2(t)\}$ is the experimental cross-correlation. The lowest sketch in Fig. 7 shows the succession of the pulses. Actually, only the time average is registered by the correlation device and there are no such separate pulses seen. They would be seen only for a case when n is very small so that each noise source would be detected separately. In deriving Eq. (10), the lower limit of integration is the larger of T_2 and $T_1 + \tau$ as shown in the sketch because, for $t < \text{larger of the two}$, one of the signals is identically zero. Therefore, in Fig. 7, the ensemble average begins at T_2 because $T_2 > T_1 + \tau$.

If $s(t)$ of the moving noise source is statistically stationary, i.e., $s(t)$ is a stationary random function, $\Psi(t_1, t_2)$ will depend only on the time difference $(t_2 - t_1)$. In Eq. (10), $(t_2 - t_1)$ is

$\{t - [r_2/c](t)\} - \{t - \tau - [r_1/c](t - \tau)\}$. However, r_1 and r_2 are still functions of t , but there is some simplification in Eq. (10) for this case. Equation (8), which applies for nonmoving sources, and Eq. (10), which applies for moving sources, are similar. The problem is to find the autocorrelation functions $\Psi(t_1, t_2)$ or $\Psi(x, \Delta t)$. In Eq. (8), $\Delta t = t_2 - t_1 = \{\tau + [r_1/c](x) - [r_2/c](x)\}$. The known quantities in Eqs. (8) or (10) are the experimental values of the cross-correlation functions which are obtained for varying microphone positions.

2. Noise Sources Moving at Supersonic Velocities

The equations for sources in supersonic motion can now also be determined. In this case, sound waves emitted by the sources at two emission times corresponding to the positions E_+ and E_- in Fig. 8 arrive at O_1 simultaneously. The region of influence of sound waves is contained within a Mach cone which moves with the source. For monopole sources, following Morse and Ingard,¹³ Eq. (9) becomes

$$p(x_1, y_1, z_1, t) = \frac{s\left(t - \frac{r_1(t)}{c}\right)}{r_1 - [M \cos \theta_1(t) - 1]^2} - \frac{s\left(t - \frac{r_2(t)}{c}\right)}{r_2 + [M \cos \theta_2(t) - 1]^2} \quad (11)$$

Equation (11) applies at distances greater than a few wavelengths from the source. The expectation value $E\{p_1(t - \tau)p_2(t)\}$ now has four terms instead of only one. These are $[s_+(\cdot) \cdot s_+(\cdot)]$, $[s_+(\cdot) \cdot s_-(\cdot)]$, $[s_-(\cdot) \cdot s_+(\cdot)]$, and $[s_-(\cdot) \cdot s_-(\cdot)]$. The observed cross-correlation is the time integral of these four terms. Thus

$$C(\tau) = n \int_{-\infty}^{\infty} E[p_1(t - \tau)p_2(t)] dt$$

with suitable upper and lower limits for the four terms.

Evaluation of the Autocorrelation Function Ψ , Based on Noise Measurements from a Subsonic Jet

In order to evaluate Ψ from Eq. (10), it is convenient to consider Ψ as a function of a time difference $\Delta t = t_2 - t_1$ and of t_2 . By referring to Eq. (10), it will be noted that if t_2 is set equal to $[t - r_2(t)/c]$, then Δt is $r_2(t)/c - r_1(t - \tau)/c + \tau$. It is also convenient to represent Ψ in the form

$$\Psi(\Delta t, t_2) = \sum_{i=1}^{N_1} g_i(t_2) \phi_i(\Delta t) \quad (12)$$

Thus, g_i is a function of t_2 only and ϕ_i is a function of Δt only. The quantity $\phi_i(\Delta t)$ is chosen to be the autocorrelation functions representing the noise in the various octave (or wider) bands N_1 . These functions are of the type¹⁴

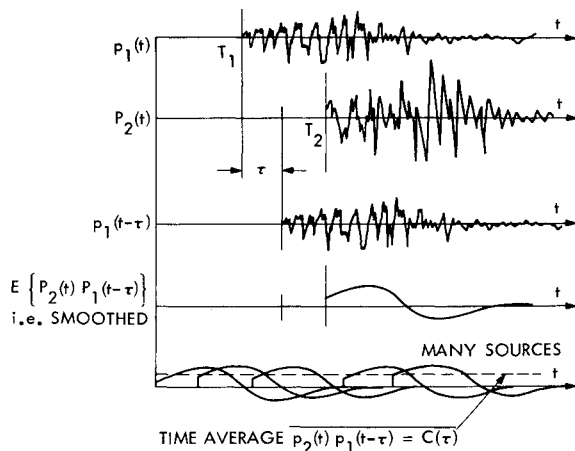


Fig. 7 Pressure fluctuations and cross-correlation of moving noise sources.

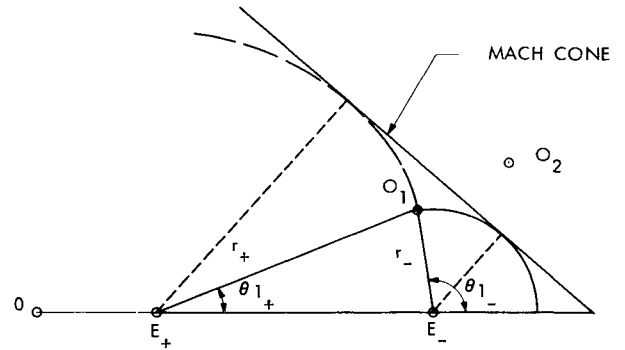


Fig. 8 A noise source in supersonic motion.

$$\phi_i(\Delta t) = \cos 2\pi f_i \Delta t \frac{\sin [(\alpha - 1)/(\alpha + 1)] 2\pi f_i \Delta t}{[(\alpha - 1)/(\alpha + 1)] 2\pi f_i \Delta t} \quad (13)$$

Thus, Eq. (13) represents an autocorrelation function for each chosen band. The frequency f_i is at the center of this band and the ratio of the highest frequency at the edge of the band to the lowest frequency is α . For an octave band, $\alpha = 2$.

The other function is Eq. (12), $g_i(t_2)$, is taken to be piece-wise linear with value $g_i(j\delta)$ defined at the nodes $0, \delta, \dots, j\delta \dots N_2\delta$ along t_2 . Therefore, in Eq. (12) there are $N_1 N_2$ unknown coefficients that must be determined to evaluate Ψ . These coefficients can be determined from a set of simultaneous equations that result from the use of Eq. (10) if known values of the cross-correlations and of the autocorrelations are introduced for $C(\tau)$.

To illustrate this method, experimental values of correlations are used which were obtained from the signals sensed by eight microphones arranged in a 60-cm-diam circle outside of a high-temperature subsonic jet as shown in Fig. 9. The jet discharged from a considerably over-expanded nozzle; hence, the flow separated inside the nozzle and, in fact, near the throat. The flow was subsonic as it emerged from the exit plane. This was verified by the absence of shock waves in a shadowgraph of the jet flow. The diameter of the jet at the nozzle exit was about 4 cm and the stagnation temperature was approximately 1090°K (1500°F). The convection velocity of the density fluctuations was determined from two-point measurements using crossed laser beams¹⁵ set up as a schlieren system. At a distance of 30 cm downstream of the nozzle exit the convection velocity was found to be 125 m/sec. This value was used in Eq. (10) and assumed to be constant.

Three frequency bands (thus $N_1 = 3$) centered at 1, 3, and 9 kHz with $\alpha = 3$ were used to evaluate $\phi_1(\Delta t)$ using Eq. (13). For $\alpha = 3$, the bandwidth is about 1.6 octaves. The time increment δ , which was used to evaluate $g_i(t_2)$ was 1.0 msec. Five increments were used which made it necessary to determine g_i at 6 nodal points; thus, N_2 was equal to 6 and, therefore, the product $N_1 N_2 = 18$ which is the number of unknown coefficients. It is, of course, evident that with such a small number of bands and nodal points the calculations in this illustrative example are crude. Nevertheless, as will be seen, the trends are reasonably good.

The correlations $C(\tau)$ shown in Fig. 9, were evaluated from the signals of the following pairs of microphones: 1 and 5, 2 and 6, 3 and 7, and 8 and 4. Also, the autocorrelation of microphone No. 1 (1, and 1 with time delay) was used. A fixed value of τ and a particular orientation of a microphone pair determine a line in the $\Delta t, t_2$ plane. The correlation $C(\tau)$ is a line integral of Ψ along this line. To get information about Ψ in various regions in this plane, different varieties of such paths (and therefore different orientations of microphones) were chosen. Points were then taken from each of these correlation curves at different values of time delay τ , thereby establishing a set of simultaneous equations. In theory only, a total of 18 values was required to evaluate the unknown coefficients; however, a

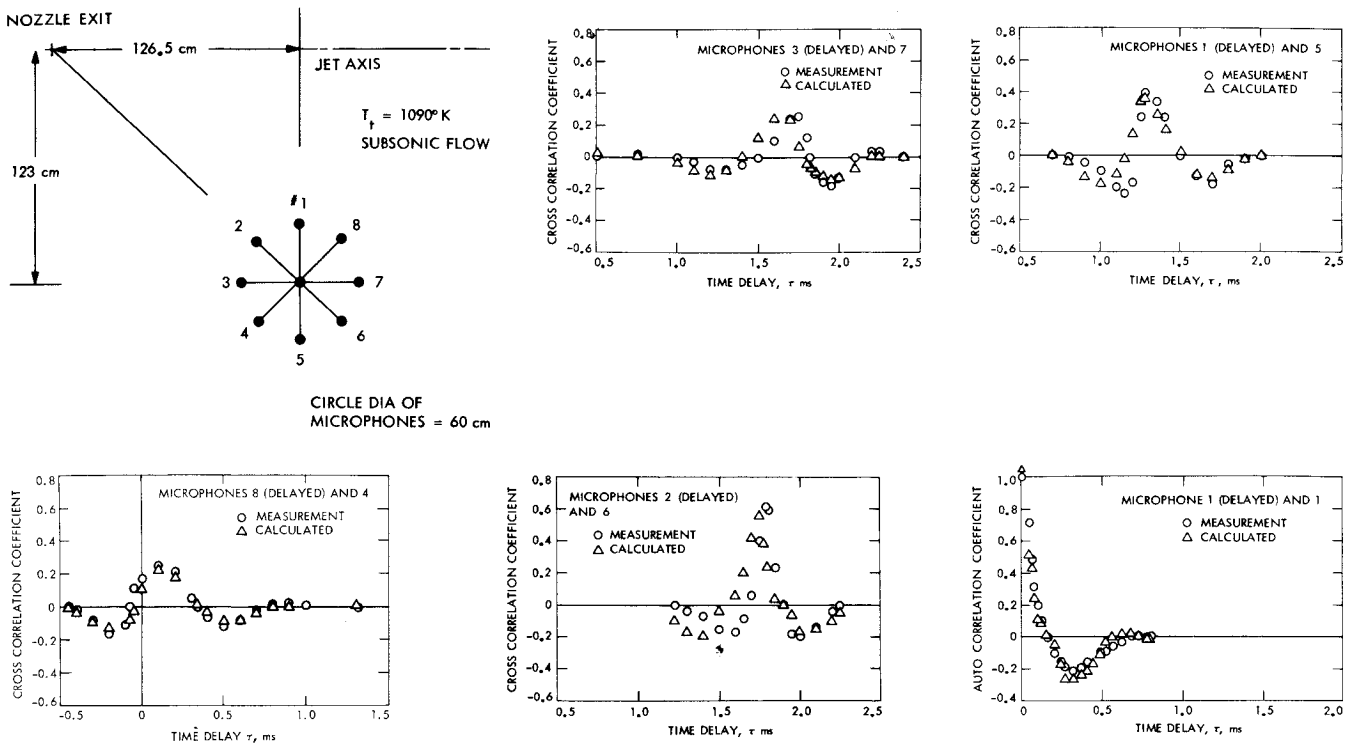


Fig. 9 Configuration of microphones and correlations.

total of about 100 was used for better smoothing since the computation method involved the use of inversion by least squares. The source function in terms of the frequency and time, i.e., $\Psi(f_i, t_2)$, obtained by this method for the three bands is shown in Fig. 10. This distribution is consistent with observed trends for subsonic jets. For example, the noise sources at higher frequencies occur near the nozzle exit and the lower frequencies extend over a larger distance along the jet.

A check on the inversion by least squares of the computation method using the coarse time step was obtained by inserting the computed coefficients into Eq. (10) and calculating values of $C(\tau)$. These computed values are shown in Fig. 9 for comparison with the experimental values. The agreement is reasonably good.

Summary and Conclusion

A theory has been presented for the evaluation of the auto-correlation function in the frame of reference of motion of noise sources from known cross-correlations. Such an evaluation would allow direct comparison of the noise sources with the statistics of flow fluctuations and with theoretical predictions relating flow fluctuations to aerodynamic noise. Such theoretical predictions are not in a refined state of development at the present time, however.

In the study presented, application of the theory to noise sources moving in a high-temperature subsonic jet indicated trends that are consistent with known characteristics of noise radiated from such flows.

Appendix : The Correlation Method for Turbulence Convecting at a Mach Number M

In jet flows, noise sources are distributed over a volume. The theory of the correlation method for point sources is extended to distributed sources. The formulation resembles in many ways the extension of Lighthill's¹⁶ theory by Ffowcs Williams.¹⁷ The theory to be discussed also yields the corresponding results for stationary sources by setting $M = 0$.

The source fluctuations may be described in terms of the old position coordinate \mathbf{Y} and emission time $t_e = t - (|\mathbf{X} - \mathbf{Y}|/c)$ or in terms of the new position $\boldsymbol{\eta} = \mathbf{Y} + \mathbf{M}[t - t_e]$ and time t . The acoustic stress tensor $T_{ij}(\mathbf{Y}, t_e)$ is transformed by substitution to $T_{ij}(\boldsymbol{\eta} - \mathbf{M}[t - t_e], t_e)$ and is denoted by $\tilde{T}_{ij}(\boldsymbol{\eta}, t_e)$ which is given in terms of the new position and old time. Quantities described in terms of $\boldsymbol{\eta}$ and t_e are indicated by a tilde in what follows.

The density fluctuation of the radiated noise at position \mathbf{X} and time $t - \tau$ is given by Lighthill's¹⁶ Eq. (32)

$$\rho'(\mathbf{X}, t - \tau) \sim \frac{1}{4\pi c^4} \int \frac{[X_i - Y_i][X_j - Y_j]}{\{|\mathbf{X} - \mathbf{Y}| - \mathbf{M} \cdot [\mathbf{X} - \mathbf{Y}]\}^3} \frac{\partial^2}{\partial t_e^2} \tilde{T}_{ij}(\boldsymbol{\eta}, t_e) d\boldsymbol{\eta} \quad (14)$$

where

$$t_e' = t_e - \tau = t - \tau - (|\mathbf{X} - \mathbf{Y}|/c)$$

A similar expression can be written for $\rho'(\mathbf{X}^*, t)$, the density fluctuation at a different position \mathbf{X}^* . The cross-correlation $\langle \rho'(\mathbf{X}, t - \tau) \rho'(\mathbf{X}^*, t) \rangle = C(\mathbf{X}, \mathbf{X}^*, \tau)$ for stationary jets and is given by the double integral

$$\frac{1}{16\pi^2 c^8} \iint \frac{[X_i - Y_i][X_j - Y_j][X_k^* - Y_k^*][X_l^* - Y_l^*]}{\{|\mathbf{X} - \mathbf{Y}| - \mathbf{M} \cdot [\mathbf{X} - \mathbf{Y}]\}^3 \{|\mathbf{X}^* - \mathbf{Y}^*| - \mathbf{M} \cdot [\mathbf{X}^* - \mathbf{Y}^*]\}^3} \times \left\langle \frac{\partial^2}{\partial t_e^2} \tilde{T}_{ij}(\boldsymbol{\eta}, t_e) \frac{\partial^2}{\partial t_e'^2} \tilde{T}_{kl}(\boldsymbol{\zeta}, t_e') \right\rangle d\boldsymbol{\eta} d\boldsymbol{\zeta} \quad (15)$$

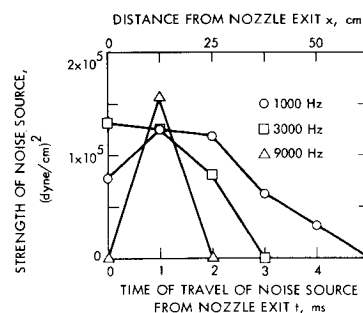


Fig. 10 Strengths of moving noise sources in various frequency bands.

where

$$\zeta = \mathbf{Y}^* + M[t - t_e^*] \quad (16)$$

$$t - t_e^* = (|\mathbf{X}^* - \mathbf{Y}^*|/c)$$

Defining

$$\langle \tilde{T}_{ij}(\boldsymbol{\eta}, t_e') \tilde{T}_{kl}(\boldsymbol{\zeta}, t_e^*) \rangle = \tilde{A}_{ijkl}(\boldsymbol{\eta}, \boldsymbol{\zeta} - \boldsymbol{\eta}, t_e^* - t_e') \quad (17)$$

the correlation of the second derivatives appearing in the previous integral becomes the fourth derivative

$$[\partial^4 / \partial(t_e^* - t_e')^4] \tilde{A}_{ijkl}(\boldsymbol{\eta}, \boldsymbol{\zeta} - \boldsymbol{\eta}, t_e^* - t_e')$$

The double integral of Eq. (15) may be evaluated over the eddy coordinate $[\boldsymbol{\zeta} - \boldsymbol{\eta}]$ first and then over the jet described in moving coordinates, $\boldsymbol{\eta}$, instead of over $\boldsymbol{\zeta}$ and $\boldsymbol{\eta}$. During integration over the eddy and over the jet cross section, which are assumed to be small compared to the length of the jet, the variation of $[\boldsymbol{\zeta} - \boldsymbol{\eta}]$ in Eq. (15) may be neglected. Let

$$\int \frac{\partial^4}{\partial(t_e^* - t_e')^4} \tilde{A}_{ijkl}(\boldsymbol{\eta}, \boldsymbol{\zeta} - \boldsymbol{\eta}, t_e^* - t_e') d[\boldsymbol{\zeta} - \boldsymbol{\eta}] = \tilde{B}_{ijkl}\left(\boldsymbol{\eta}, \tau - \frac{|\mathbf{X}^* - \mathbf{Y}|}{c} + \frac{|\mathbf{X} - \mathbf{Y}|}{c}\right) \quad (18)$$

Then the cross-correlation

$$C(\mathbf{X}, \mathbf{X}^*, \tau) = \frac{1}{16\pi^2 c^8} \int \frac{[X_i - Y_i][X_j - Y_j][X_k^* - Y_k^*][X_l^* - Y_l^*]}{\{|\mathbf{X} - \mathbf{Y}| - M \cdot [\mathbf{X} - \mathbf{Y}]\}^3 \{|\mathbf{X}^* - \mathbf{Y}| - M \cdot [\mathbf{X}^* - \mathbf{Y}]\}^3} \times \tilde{B}_{ijkl}\left(\boldsymbol{\eta}, \tau - \frac{|\mathbf{X}^* - \mathbf{Y}|}{c} + \frac{|\mathbf{X} - \mathbf{Y}|}{c}\right) d\boldsymbol{\eta} \quad (19)$$

Returning to the old coordinate \mathbf{Y} , any integral $\int f(\boldsymbol{\eta}) d\boldsymbol{\eta}$ transforms to

$$\int f(\boldsymbol{\eta}(\mathbf{Y})) \left\{ \frac{|\mathbf{X} - \mathbf{Y}| - M \cdot [\mathbf{X} - \mathbf{Y}]}{|\mathbf{X} - \mathbf{Y}|} \right\} d\mathbf{Y}$$

The additional factor that appears is the Jacobian of the transformation. Thus, Eq. (19) gives

$$C(\mathbf{X}, \mathbf{X}^*, \tau) = \frac{1}{16\pi^2 c^8} \times \int \frac{[X_i - Y_i][X_j - Y_j][X_k^* - Y_k^*][X_l^* - Y_l^*]}{\{|\mathbf{X} - \mathbf{Y}| - M \cdot [\mathbf{X} - \mathbf{Y}]\}^2 |\mathbf{X} - \mathbf{Y}| \{|\mathbf{X}^* - \mathbf{Y}| - M \cdot [\mathbf{X}^* - \mathbf{Y}]\}^3} \times B_{ijkl}\left(\mathbf{Y}, \tau - \frac{|\mathbf{X}^* - \mathbf{Y}|}{c} + \frac{|\mathbf{X} - \mathbf{Y}|}{c}\right) d\mathbf{Y} \quad (20)$$

where

$$B_{ijkl}(\mathbf{Y}, t) = \tilde{B}_{ijkl}(\boldsymbol{\eta}, t) \quad (21)$$

The next integration is over the area of cross section during which Y_i may be replaced by the position vector $Y_{1i} = (Y_1, 0, 0)$. The direction cosines, L_i and L_j^* together with the angles θ and θ^* and C_{ijkl} are introduced as follows:

$$L_i = \frac{X_i - Y_i}{|\mathbf{X} - \mathbf{Y}_1|}, \quad L_j^* = \frac{X_j^* - Y_{1j}}{|\mathbf{X}^* - \mathbf{Y}_1|}$$

$$\cos \theta = \frac{M \cdot [\mathbf{X} - \mathbf{Y}_1]}{|\mathbf{X} - \mathbf{Y}_1|}, \quad \cos \theta^* = \frac{M \cdot [\mathbf{X}^* - \mathbf{Y}_1]}{|\mathbf{X}^* - \mathbf{Y}_1|} \quad (22)$$

$$C_{ijkl}\left(Y_1, \tau - \frac{|\mathbf{X}^* - \mathbf{Y}_1|}{c} + \frac{|\mathbf{X} - \mathbf{Y}_1|}{c}\right) = \int B_{ijkl}\left(\mathbf{Y}_1, \tau - \frac{|\mathbf{X}^* - \mathbf{Y}_1|}{c} + \frac{|\mathbf{X} - \mathbf{Y}_1|}{c}\right) dY_2 dY_3$$

The cross-correlation then becomes

$$C(\mathbf{X}, \mathbf{X}^*, \tau) = \frac{1}{16\pi^2 c^8} \int_{Y_1=0}^{\infty} \frac{L_i L_j L_k^* L_l^*}{|\mathbf{X} - \mathbf{Y}_1| |\mathbf{X}^* - \mathbf{Y}_1| [1 - M \cos \theta]^2 [1 - M \cos \theta^*]^3} \times C_{ijkl}\left(Y_1, \tau - \frac{|\mathbf{X}^* - \mathbf{Y}_1|}{c} + \frac{|\mathbf{X} - \mathbf{Y}_1|}{c}\right) dY_1 \quad (23)$$

This agrees in content with Eq. (10) for point sources in motion. For $M = 0$, it agrees with Eq. (8) for stationary sources. The differences are due to the presence of directional cosines and the power of $[1 - M \cos \theta^*]$ being 3 instead of 2, both of which arise in the quadrupole formulation.

The numerical factor $1/16\pi^2 c^8$ was partly absorbed in the definition of the source strength in the point source formulation. In Eq. (23), $C(\mathbf{X}, \mathbf{X}^*, \tau)$ represents the cross-correlation of the density field and is therefore equal to $1/c^4$ times the cross-correlation of pressures.

In the moving source formulation, the cross-correlation was obtained as an integral over the reception time. This transformation can be made by using the relations

$$t - t_e = (|\mathbf{X} - \mathbf{Y}_1|/c) \quad (24)$$

$$Y_1 = V t_e$$

By eliminating t_e

$$t - (Y_1/V) = (|\mathbf{X} - \mathbf{Y}_1|/c) \quad (25)$$

which gives on differentiation

$$dt - \frac{dY_1}{V} = \frac{d|\mathbf{X} - \mathbf{Y}_1|}{c} = - \frac{dY_1 \cos \theta}{c}$$

i.e.,

$$dY_1 = \frac{V dt}{1 - M \cos \theta} \quad (26)$$

Therefore,

$$C(\mathbf{X}, \mathbf{X}^*, \tau) = \frac{1}{16\pi^2 c^8} \int_{Y_1}^{\infty} \frac{L_i L_j L_k^* L_l^*}{|\mathbf{X} - \mathbf{Y}_1| |\mathbf{X}^* - \mathbf{Y}_1| [1 - M \cos \theta]^3 [1 - M \cos \theta^*]^3} \times C_{ijkl}\left(\mathbf{Y}_1, \tau - \frac{|\mathbf{X}^* - \mathbf{Y}_1|}{c} + \frac{|\mathbf{X} - \mathbf{Y}_1|}{c}\right) V dt \quad (27)$$

In the previous integrand, Y_1, θ, θ^* are functions of t . Equation (27) corresponds to Eq. (10) closely, the differences again being due to the quadrupole nature of the sources as stated after Eq. (23).

From the preceding analysis, the relation between the quadrupole distribution and the point source model is clear. The moving autocorrelation of the point source is the autocorrelation of the distributed quadrupole sources, integrated over the eddy and again over the area of cross section of the jet. The quadrupoles have a basic directionality and a random distribution of such quadrupoles is probably only mildly directional. If so, the omni-directional point source can approximate the quadrupoles well. If not, the basic directionality may be accounted for by formulating a moving point quadrupole model by introducing the directionality factor $L_i L_j$ into Eq. (9) and changing the power of $[1 - M \cos \theta]$ from 2 to 3.

References

- Mason, W. P. and Marshall, R. N., "A Tubular Directional Microphone," *Journal of the Acoustical Society of America*, Vol. 10, July-April 1938-39, pp. 206-215.
- Grosche, F. R., "Measurements of the Noise of Air Jets from Slot Nozzles With and Without Shields," *Deutsche Luft- und Raumfahrt, Forschungsbericht* 68-46, July 1968, pp. 1-30.
- Lighthill, M. J., "On Sound Generated Aerodynamically. II. Turbulence As A Source of Sound," *Proceedings of the Royal Society, A*, Vol. 222, 1954, pp. 1-32.
- Gerrard, J. H., "An Investigation of the Noise Produced by a Subsonic Air Jet," *Journal of the Aerospace Sciences*, Vol. 23, 1956, pp. 855-866.
- Westley, R. and Lilley, G. M., "An Investigation of the Noise Field from a Small Jet and Methods for its Reduction," Rept. 53, 1952, College of Aeronautics, Cranfield, England.
- Yu, J. C. and Dosanjh, D. S., "Noise Field of Coaxial Interacting Supersonic Jet Flows," AIAA Paper 71-152, New York, 1971.
- Tam, C. K. W., "On the Noise of a Nearly Ideally Expanded

Supersonic Jet," *Journal of Fluid Mechanics*, Vol. 51, Pt. 1, 1972, pp. 69-95.

⁸ Bishop, K. A., Ffowcs Williams, J. E., and Smith, W., "On the Noise Sources of the Unsuppressed High-Speed Jet," *Journal of Fluid Mechanics*, Vol. 50, Pt. 1, 1971, pp. 21-31.

⁹ Dyer, I., "Distribution of Sound Sources in a Jet Stream," *The Journal of the Acoustical Society of America*, Vol. 31, No. 7, July 1959, pp. 1016-1022.

¹⁰ Howes, W. L. and Mull, H. R., "Near Noise Field of a Jet Engine Exhaust. I. Sound Pressures," TN 3765, 1956, NACA.

¹¹ Maestrello, L. and McDaid, E., "Acoustic Characteristics of a High-Subsonic Jet," *AIAA Journal*, Vol. 9, No. 6, June 1971, pp. 1058-1066.

¹² Mollo-Christensen, E., "Jet Noise and Shear Flow Instability

Seen from an Experimenter's Viewpoint," *Journal of Applied Mechanics*, March 1967, pp. 1-7.

¹³ Morse, P. M. and Ingard, U. K., *Theoretical Acoustics*, McGraw-Hill, New York, 1968, pp. 717-727.

¹⁴ Lange, F. H., *Correlation Techniques*, D. Van Nostrand, Princeton, N.J., 1967, pp. 167-168.

¹⁵ Fisher, M. J. and Krause, F. R., "The Crossed-Beam Correlation Technique," *Journal of Fluid Mechanics*, Vol. 28, Pt. 4, pp. 705-717.

¹⁶ Lighthill, M. J., "On Sound Generated Aerodynamically. I. General Theory," *Proceedings of the Royal Society, A*, Vol. 211, 1952, pp. 564-587.

¹⁷ Ffowcs Williams, J. E., "The Noise from Turbulence Convected at High Speed," *Royal Society of London, Philosophical Transactions, Series A*, Vol. 255, 1962-63, pp. 469-502.

MAY 1974

AIAA JOURNAL

VOL. 12, NO. 5

Method for Calculating Unsteady Turbulent Boundary Layers in Two- and Three-Dimensional Flows

ROBERT E. SINGLETON*

Army Research Office, Durham, N.C.

AND

JOHN F. NASH†

Scientific & Business Consultants, Inc., Atlanta, Ga.

The governing equations for an unsteady turbulent boundary layer on a swept infinite cylinder, composed of a continuity equation, a pair of momentum equations and a pair of rate equations for the shear stress, based on the turbulent kinetic-energy equation, are solved numerically. These rate equations for the shear stress express a balance between the convection, production, dissipation and diffusion of the turbulent shear stress components. Due to the physical model of turbulence employed, this system of equations is hyperbolic. An explicit, second-order accurate, conditionally stable difference scheme for this system, together with appropriate boundary and initial conditions, is formulated and developed into a computer program. Calculations for oscillating freestream flows with no pressure gradient show significant unsteady effects on the turbulent boundary layer. Expected phase shifts in wall shear stress and displacement thickness were found, as observed by other investigators. The quasi-steady wall shear stress values were a good approximation to the corresponding unsteady values for the entire frequency range considered. However, for these same frequency ranges, the same cannot be said of the displacement thickness values. The displacement thickness was not represented well by the quasi-steady model even at relatively low frequencies.

I. Introduction

THE role of unsteadiness, in many current fluid-mechanics problems, is of obvious importance, but at the same time, the subject of unsteady turbulent boundary layers has attracted few investigators. An important example of this situation is the flow over a helicopter rotor in translating motion. Preliminary investigations of this unsteady problem area¹ demonstrated the need to study the effects of time-dependence in rotor aero-

dynamics. Of course, dynamic stall affects, not only helicopter rotors, but also the blades of turbines and compressors, and the aerodynamic surfaces of maneuvering aerodynamic vehicles. Furthermore, the subject is of substantial fundamental interest, and a greater understanding of it would necessarily assist in the understanding of a much wider range of boundary-layer flows.

The subject of unsteady turbulent boundary layers is in its infancy. The differential method of Patel and Nash² and the integral method of McDonald and Shamroth³ for calculating two-dimensional flows with both spatial and temporal variations were recently published. A few other methods have also appeared which treat only temporally-varying flows.^{4,5}

The method presented in this paper is a further development of the method of Patel and Nash and an extension of their method to infinite-yawed-cylinder flows. A brief description is given of the governing equations, the turbulence model used and the necessary assumptions made. Details of the numerical method are described and illustrated by several example calculations,

Presented at the AIAA Computational Fluid Dynamics Conference, Palm Springs, Calif., July 19-20, 1973; submitted July 25, 1973; revision received November 26, 1973. This research was supported by Contract NAS2-6466 with the U.S. Army Air Mobility Research and Development Lab., Ames Research Center, Moffett Field, Calif.

Index categories: Boundary Layers and Convective Heat Transfer—Turbulent; Nonsteady Aerodynamics.

* Chief, Fluid Mechanics Branch.

† Staff.